

## Selective Oxidation of Alkenes by Dioxygen Using Modified Gold Nanoclusters

H. Salari<sup>a,\*</sup> and M.R. Gholami<sup>b</sup>

<sup>a</sup>Department of Chemistry, College of Sciences, Shiraz University, Shiraz, Iran

<sup>b</sup>Department of Chemistry, Sharif University of Technology, Tehran, Iran

(Received 21 February 2020, Accepted 2 June 2020)

Selective oxidation of cyclohexene and styrene was investigated using molecular oxygen under mild conditions. The Au/TiO<sub>2</sub> and Au/Al<sub>2</sub>O<sub>3</sub> surfaces were impregnated with three different ionic liquids. Supported ionic liquids (ILs) gold nanocatalysts are particularly versatile catalysts for oxidation reactions with exceptionally high efficiency and significant selectivity. Improved activity is attributed to the stabilization of the reaction intermediates *via* different interactions such as hydrogen bonding and polarity/dipolarizability between ILs and intermediates. Surface coating of obtained nanoparticles with ionic liquids is found to increase the interaction energy. The estimated rate constant decreases in the following order: [EAP] > [bmim]PF<sub>6</sub> > [emim]EtSO<sub>4</sub>. The EAP/Au/Al<sub>2</sub>O<sub>3</sub> surface exhibited maximum conversion compared to other ILs-impregnated catalysts. Supported ionic liquids gold nanocatalysts are active catalysts for oxidation reaction with high efficiency and selectivity.

**Keywords:** Oxidation reaction, Molecular oxygen, Gold nanoparticles

### INTRODUCTION

In green and sustainable chemistry, molecular oxygen is recognized as an ideal oxidant because of its natural, inexpensive and environmentally friendly properties. Molecular oxygen in heterogeneous metal catalyzed oxidation reaction is limited with three fundamental points: incomplete reaction achieved in the absence of a cocatalyst, difficulty in oxidation reactions at mild condition, and low chemoselectivity of oxidation reaction. In recent years, selective oxidation reaction with dioxygen has been developed [1-4]. Friend *et al.* [5] studied the reversible oxidation of styrene with dioxygen on Au(111) lattice in high temperature. Accordingly, the styrene epoxidation reaction should be performed at low temperature to achieve high activity. M. Turner and coworkers reported the effectiveness of small gold nanoparticles (~1.4 nm) supported on SiO<sub>2</sub>, C and BN as catalyst for selective oxidation of styrene by dioxygen [6]. They represented

~2 nm particle size as a main threshold in catalytic activity. Hughes *et al.* have explored high activity of oxygen activated gold nanocrystals in selective oxidation of cyclohexene and cis-cyclooctene [7]. Supported gold as a new source of catalyst for oxidation of alcohols and alkenes showed improvement in selectivity and stability. Because of compatibility, recovery and availability, gold appears as an exciting catalyst for important processes in aqueous solution under mild conditions. When gold is deposited as small nanoparticles on some selected group of metal oxides, it shows high activity and selectivity. Although the origin of gold catalytic activity is not fully understood, it proposes the interactions of gold and support as a main reason [6,7]. Particles size, which is influenced by the synthesis method of catalyst, plays an important role in particles and metal-support interactions. Ultrafine particles (clusters) with dimension below ~10 nm, supported on thin metal oxide films, exhibited extraordinary catalytic activity. A sharp maximum in the catalytic activity was observed at a particle size about 3 nm that is attributed to the opening of an energy gap in the electronic density of states of the Fermi

\*Corresponding author. E-mail: [hsalari@shirazu.ac.ir](mailto:hsalari@shirazu.ac.ir)

level [7-10]. The oxidation of alkenes is often inefficient and these types of reactions lead to fine chemical intermediates usable for manufacture of high value pharmaceuticals. Although ample progress has been made in this regard, low efficiency of the system is considered as a main drawback associated with the heterogeneous oxidation reactions [6,7]. Ionic liquids (ILs) are organic salts known as a new class of solvents with applied properties [9,11]. Low volatility, stability, reusability and easy handling are some of the practical features of ionic liquids. They have wide attractive applications in separation, catalysis, synthesis and extraction [12-17]. ILs play an important role as cosolvent in binary and ternary solvent mixture systems [9,10,18]. ILs in liquid-liquid biphasic catalytic system provide an alternative medium for dissolving the substrate and stabilization of intermediates. ILs as a thin film layer on the surface simplify the diffusion of species in two phase reactions. ILs could be located on the surface of catalysts strongly because of hydrogen bonding interactions or covalent anchoring [19-23].

## EXPERIMENTAL

### Catalysts Preparation

Au/TiO<sub>2</sub> and Au/Al<sub>2</sub>O<sub>3</sub> were prepared by homogeneous deposition-precipitation (HDP) using urea as the precipitation agent. The decanted solid samples were washed several times with hot water and dried for 12 h at 80 °C. The materials were calcined at 500 °C under static air for 2 h. The obtained catalysts were modified by some ionic liquids (buthylmethylimidazolium hexafluorophosphate ([bmim]PF<sub>6</sub>), ethylmethylimidazolium ethylsulfate ([bmim]EtSO<sub>4</sub>), and ethylammonium propionate (EAP)) with impregnation of 30% W of IL to support. Impregnation of 30 wt% ionic liquid onto the support surface was performed in ethanol solution in an ultrasonic bath for 10 min followed by ethanol evaporation under reduced pressure at room temperature.

### Catalytic Reaction

The oxidation reaction of alkenes over the catalysts was carried out at 0.1 MPa pressure of oxygen gas by contacting 0.03 g catalyst with 0.7 ml alkenes in 15 ml solvent in a stirred batch reactor (capacity: 50 cm<sup>3</sup>), under reflux (at 78-

80 °C) and vigorously stirring for a period of 24 h. The reaction products and unconverted reactants were analyzed by GC with FID using HP5 column and He as the carrier gas. After completion of the reaction, the reaction mixture was filtered off and the catalyst rinsed three times with ethanol, the excess of solvent was then removed under reduced pressure.

### Characterization

Characterization of the catalysts was conducted by different physicochemical methods. The synthesized Au/TiO<sub>2</sub> and Au/Al<sub>2</sub>O<sub>3</sub> were characterized by X-ray diffraction (XRD- X-ray diffractometer, PANalytical X'Pert-Pro) with a Cu-K<sub>α</sub> monochromatized radiation source and a Ni filter), X-ray photoelectron spectroscopy (XPS-Bestec) and transmission electron microscopy (TEM, Philips Tecnai G220, operated at 120 kV). Morphological investigations of the prepared samples were carried out by scanning electron microscopy (SEM- KYKY-EM3200). Thermogravimetric analysis (TGA) and differential scanning calorimetry (DSC) were performed with SDT Q-600. Fourier transform infrared (FTIR- Thermo avatar) was employed for organic functionalized group identifying.

## RESULTS AND DISCUSSION

The SEM images (Fig. 1) show that ILs were impregnated on catalysts surfaces. The crystalline properties of Au/Al<sub>2</sub>O<sub>3</sub> and Au/TiO<sub>2</sub> were investigated by XRD. The XRD patterns of the Au/Al<sub>2</sub>O<sub>3</sub> and Au/TiO<sub>2</sub> (Fig. 2) show that Au(111) was formed selectively on Al<sub>2</sub>O<sub>3</sub>. Sharp diffraction peaks at 2θ = 38, 48 and 63 are related to (111), (200) and 220 of Au in Au/TiO<sub>2</sub>, respectively. The peaks at 2θ = 45 and 67 correspond to (400) and (440) planes of δ-Al<sub>2</sub>O<sub>3</sub>. Two peaks at 2θ = 25 and 28 representing characteristic peaks of anatase and rutile in P25. The TGA and DTG analyses of catalysts, depicted in Fig. 3, demonstrate that 30% of catalysts include ILs. The FT-IR spectra of synthesized Au/TiO<sub>2</sub> and Au/Al<sub>2</sub>O<sub>3</sub> and impregnated catalysts are shown in Fig. 4. The sharp band at 930 cm<sup>-1</sup> was attached to Ti-O stretching vibration. With impregnation of ILs on the metal oxides surfaces, new peaks were appeared in FTIR spectra of catalysts. Symmetric stretching bend of imidazole ring was observed

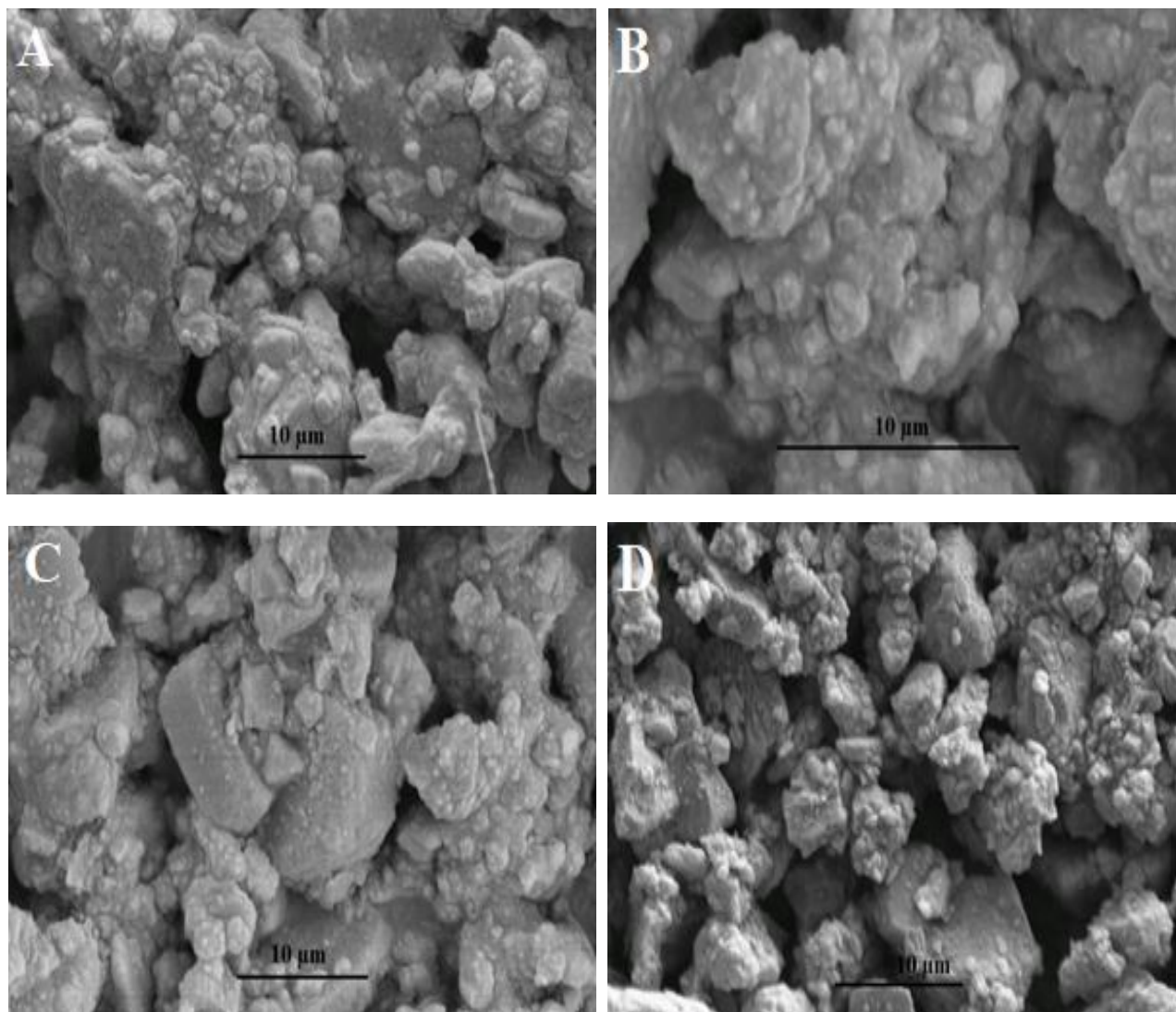


**Fig. 1.** SEM images of IL/Au/Al<sub>2</sub>O<sub>3</sub> (A,B) and IL/Au/TiO<sub>2</sub> (C,D).

around 1430 and 1570 cm<sup>-1</sup>. In the region 2500-4000 cm<sup>-1</sup>, C-H stretching vibrations were observed. The peak over 3100 cm<sup>-1</sup> in the spectrum can be attributed to the ring C-H stretch while below 3000 cm<sup>-1</sup> can be related to aliphatic stretches.

The TEM images of Au/Al<sub>2</sub>O<sub>3</sub> and Au/TiO<sub>2</sub> are presented in Fig. 5. As can be seen, Au nanoparticles were distributed uniformly on Al<sub>2</sub>O<sub>3</sub> and TiO<sub>2</sub> surface by the average size of ~ 8 nm. The chemical states of elements and

surface composition can be analyzed by XPS. The XPS spectrum of Au/Al<sub>2</sub>O<sub>3</sub> and Au/TiO<sub>2</sub> are demonstrated in Figs. 6 and 7. The presence of Ti, O, Au and Al atoms was detected by scanning the nanostructure. After de-convolution of gold (Au4f), two peaks appeared at 82.9 and 85.2 eV for Au/Al<sub>2</sub>O<sub>3</sub> and at 83.5 and 86 eV for Au/TiO<sub>2</sub>, respectively. The first and second peaks correspond to 4f<sub>7/2</sub> and 4f<sub>5/2</sub>, respectively. The high resolution spectra of oxygen (O1s) are centered at 532.5 eV

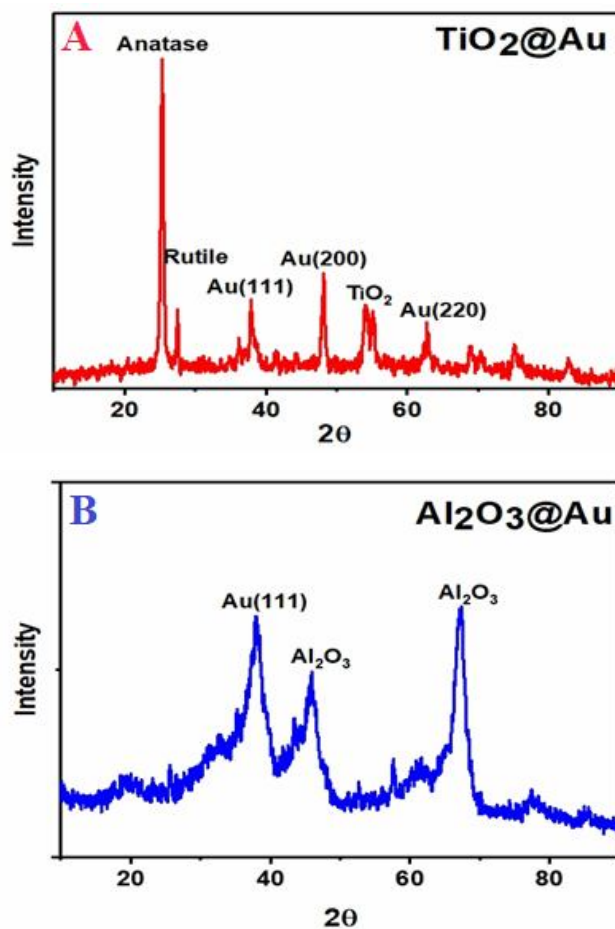


Fig. 2. XRD patterns of Au/Al<sub>2</sub>O<sub>3</sub> (A) and Au/TiO<sub>2</sub> (B).

for Au/Al<sub>2</sub>O<sub>3</sub> and 536.0 eV for Au/TiO<sub>2</sub>, respectively. It should be emphasized that shifting of binding energy in oxygen and gold is due to the different electronic interactions in Au/Al<sub>2</sub>O<sub>3</sub> and Au/TiO<sub>2</sub> hetero-structures. The peak with binding energy of 74.3 eV is attributed to Al2p in Au/Al<sub>2</sub>O<sub>3</sub>. The binding energy of Ti2p is centered at 464 eV and 467 eV, related to 2p<sub>3/2</sub> and 2p<sub>1/2</sub>.

Using supported ILS gold catalysts, a high efficiency with visible selectivity was achieved (Scheme 1). Tables 1 and 2 summarize the performance of Au catalysts at 80 °C using toluene solvent for the partial oxidation of cyclohexene and styrene. The weight percents of Au loading on the metal oxides supports are 1%. The oxidation reaction has been performed in a three-phase catalytic system.

Toluene has been selected as a solvent due to two points: high solubility of O<sub>2</sub>, and immiscibility in ILS. The comparison study between the supported and unsupported gold catalysts showed that the catalysts with ionic liquid thin film exhibit a slightly enhanced activity with a comparable selectivity. The catalytic conversions were 45 and 23 for Au@Al<sub>2</sub>O<sub>3</sub> and Au@TiO<sub>2</sub> in cyclohexene oxidation as well as 15 and 14 for Au@Al<sub>2</sub>O<sub>3</sub> and Au@TiO<sub>2</sub> in styrene oxidation, respectively. The catalytic activities were ranked as follows: EAP/Au/MO > [bmim]PF<sub>6</sub>/Au/MO > [emim]EtSO<sub>4</sub>/Au/MO (MO is metal oxide). Based on the results reported in Tables 1 and 2, the activity of Au/TiO<sub>2</sub> is higher than that of Au/Al<sub>2</sub>O<sub>3</sub> for styrene oxidation.

It should be also point out that Au/Al<sub>2</sub>O<sub>3</sub> reveals higher

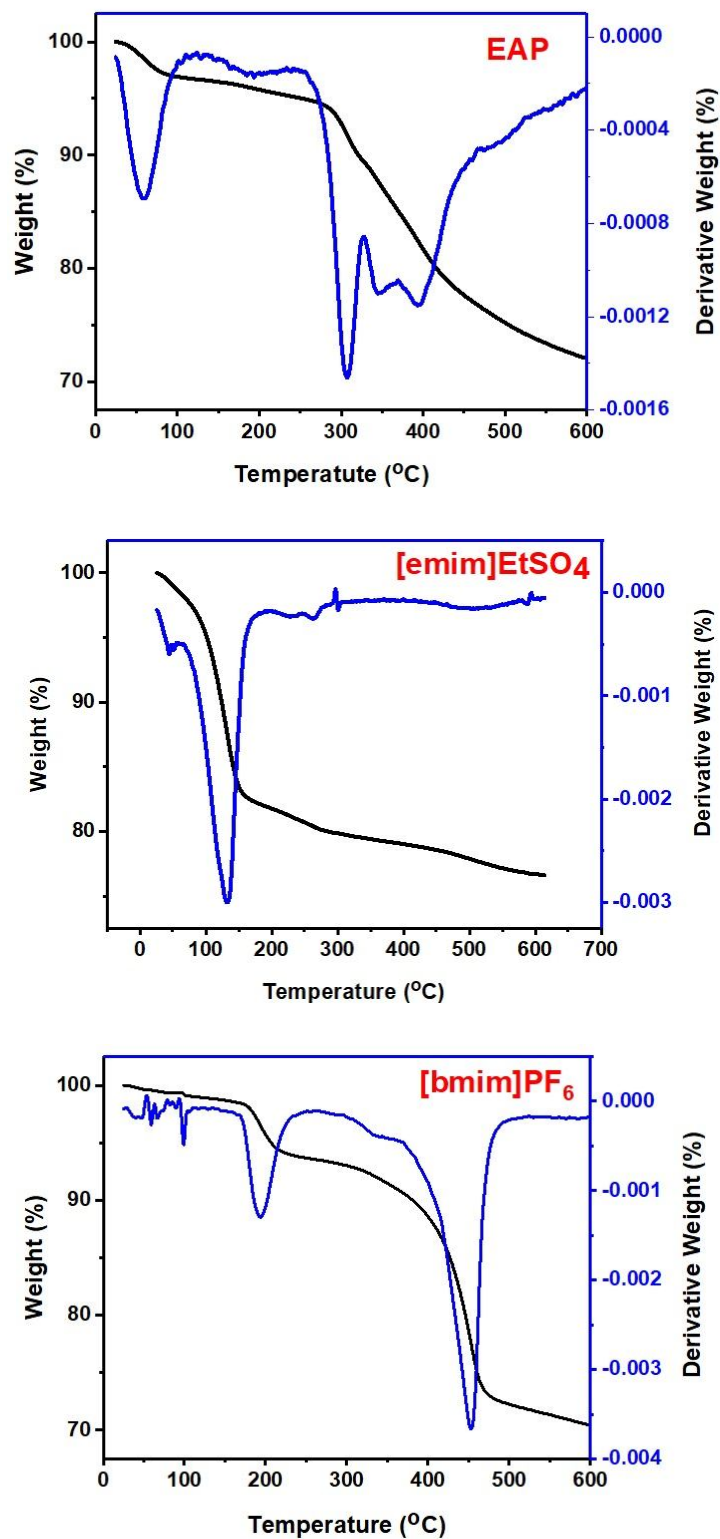


**Fig. 3.** TGA and DSC analyses of catalysts with three impregnated ionic liquids.

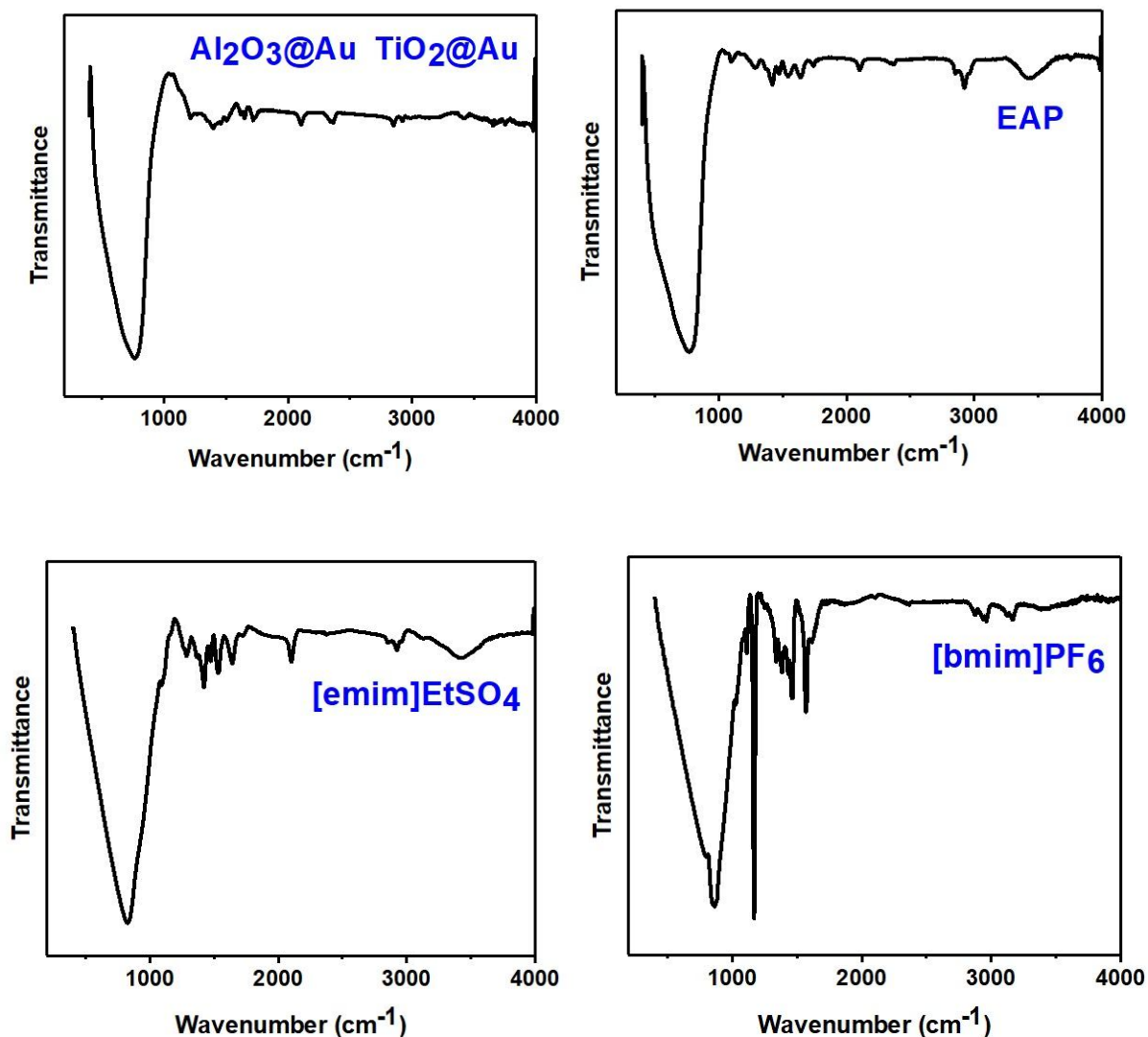


Fig. 4. IR spectrum of three impregnated ionic liquids.

conversion of cyclohexene compared to Au/TiO<sub>2</sub>, and that addition of ILs to gold catalysts is associated with a higher turnover frequency (TOF) and conversion in all cases. This improved activity might be attributed to the stabilization of reaction intermediates *via* different interactions such as hydrogen bonding and polarity/dipolarizability between ILs and intermediates. Despite diffusion limit of oxygen and substrate to the catalyst surface, these observations show that supported gold nanoparticles could adsorb and activate O<sub>2</sub>. With dissociation of O<sub>2</sub> to O atoms the catalytic

oxidation reaction is initiated [24,25]. The turnover frequency of catalysts is strongly related to the size of gold particles. Only small gold particles are active for liquid phase oxidation of alcohols and alkenes [26]. This catalytic system exhibited that gold intrinsically catalyzes the reaction and dissociation of O<sub>2</sub> bond occurring in the surface of nanoparticles and common interface between nanoparticles and support. Unexpected catalytic activity of the nanoscaled Au system is due to the quantum size effects in the electronic structures caused by electron confinement



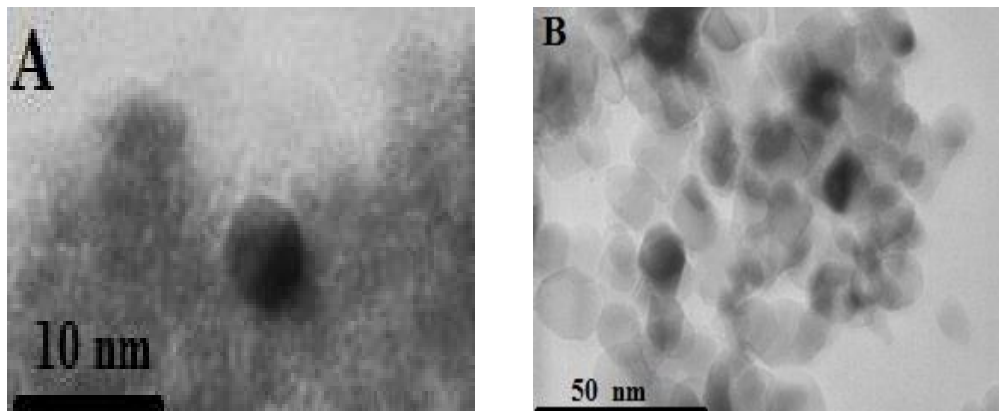


Fig. 5. TEM images of IL/Au/Al<sub>2</sub>O<sub>3</sub> (A) and IL/Au/TiO<sub>2</sub> (B).

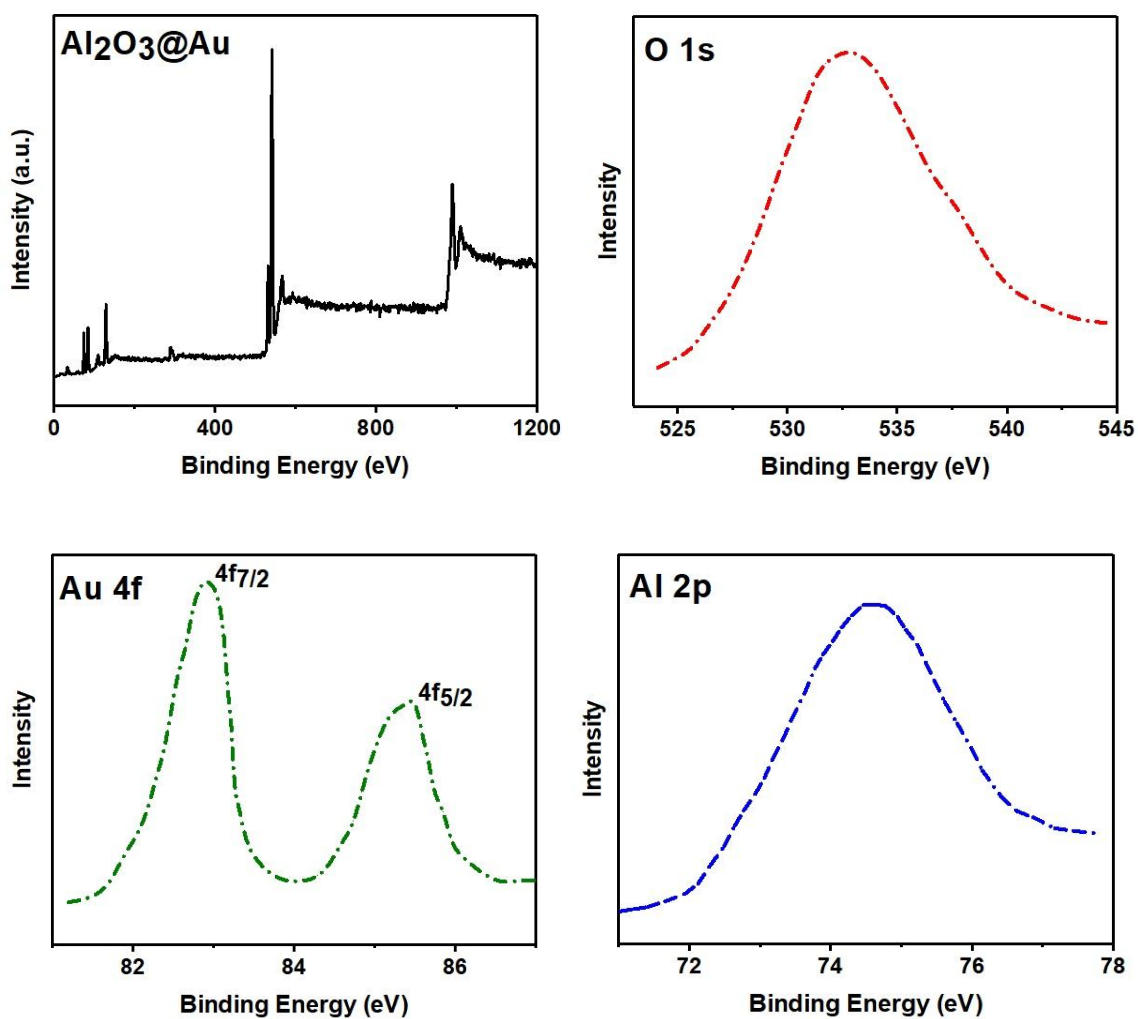


Fig. 6. XPS analysis of Au/Al<sub>2</sub>O<sub>3</sub>.

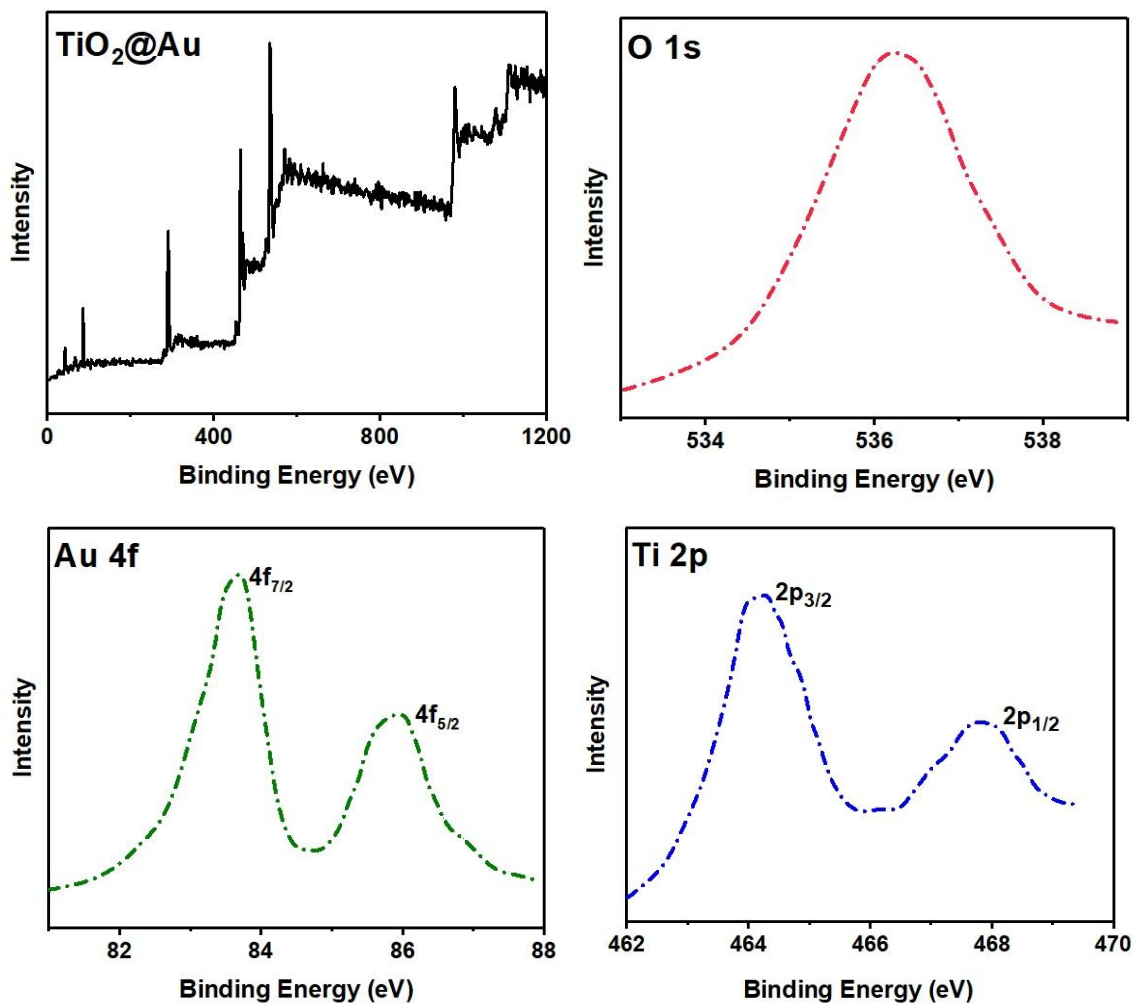
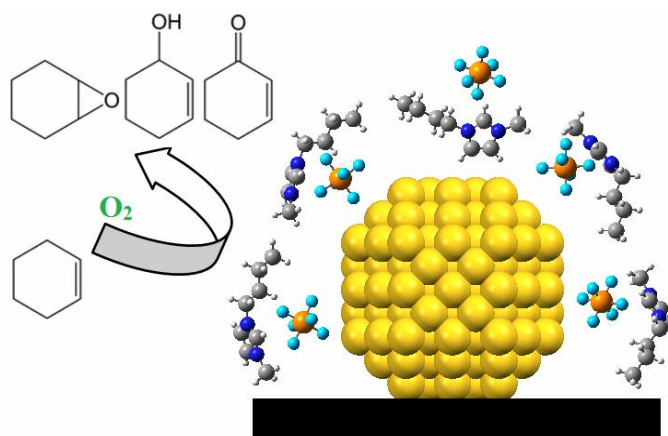


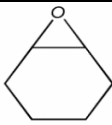
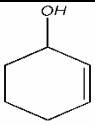
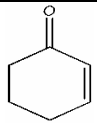
Fig. 7. XPS analysis of Au/TiO<sub>2</sub>.



Scheme 1. Selective oxidation of cyclohexene with molecular oxygen by supported ionic liquid gold nanoclusters

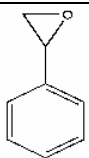
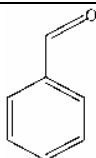
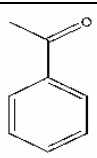


**Table 1.** Catalytic Results of Cyclohexene Oxidation with Molecular Oxygen

Catalyst	Conversion (%)	$\sum_{\text{SeI}}\text{C}_6^{\text{a}}$	TON	TOF (h <sup>-1</sup> )	Selectivity (%)		
							
[bmim]PF <sub>6</sub> /Al <sub>2</sub> O <sub>3</sub>	4	-	-	-	-	-	
Au/Al <sub>2</sub> O <sub>3</sub>	30	98	23546	9987	33.3	32.8	33.8
[bmim]PF <sub>6</sub> /Au/Al <sub>2</sub> O <sub>3</sub>	60	97	47280	19700	22.5	34.3	43.1
EAP/Au/Al <sub>2</sub> O <sub>3</sub>	70	97	55160	22983	18.5	35.7	45.6
[emim]EtSO <sub>4</sub> /Au/Al <sub>2</sub> O <sub>3</sub>	58	96	45704	19043	20	35	43
[bmim]PF <sub>6</sub> /TiO <sub>2</sub>	2	-	-	-	-	-	-
Au/TiO <sub>2</sub>	26	97	31435	7054	32.6	33	34.1
[bmim]PF <sub>6</sub> /Au/TiO <sub>2</sub>	39	96	30732	12805	18	35	45
EAP/Au/TiO <sub>2</sub>	45	97	35460	14775	23	33	43
[emim]EtSO <sub>4</sub> /Au/TiO <sub>2</sub>	41	96	32308	13461	22	34.3	41.8

<sup>a</sup>Total selectivity to C<sub>6</sub> products.

**Table 2.** Catalytic Results of Styrene Oxidation with Molecular Oxygen

Catalyst	Conversion (%)	$\sum_{\text{SeI}}\text{C}_7^{\text{a}}$	TON	TOF (h <sup>-1</sup> )	Selectivity (%)		
							
[bmim]PF <sub>6</sub> /Al <sub>2</sub> O <sub>3</sub>	3	-	-	-	-	-	
Au/Al <sub>2</sub> O <sub>3</sub>	13	97	9234	3765	33.2	32.9	33.7
[bmim]PF <sub>6</sub> /Au/Al <sub>2</sub> O <sub>3</sub>	26	98	18148	7562	22	34	44
EAP/Au/Al <sub>2</sub> O <sub>3</sub>	31	97	21638	9016	17	37	45
[emim]EtSO <sub>4</sub> /Au/Al <sub>2</sub> O	22	97	15356	6398	19	36	44
[bmim]PF <sub>6</sub> /TiO <sub>2</sub>	2	-	-	-	-	-	-
Au/TiO <sub>2</sub>	17	98	10123	4432	32	33.8	34.1
[bmim]PF <sub>6</sub> /Au/TiO <sub>2</sub>	31	96	21638	9159	17	36	45
EAP/Au/TiO <sub>2</sub>	40	97	27920	11633	20	36	43
[emim]EtSO <sub>4</sub> /Au/TiO <sub>2</sub>	27	94	18846	7852	21	33	42

<sup>a</sup>Total selectivity to C<sub>7</sub> products.

**Table 3.** Solvatochromic Parameters for Three Ionic Liquids

IL	$E_T^N$	$\pi^*$	$\beta$	$\alpha$
EAP <sup>10</sup>	0.85	0.79	0.91	1.18
[bmim]PF <sub>6</sub> [28]	0.67	1.03	0.21	0.63
[emim]EtSO <sub>4</sub> [29]	0.68	0.98	0.78	0.76

to a restricted volume. Many of metallic elements dissociatively chemisorb O<sub>2</sub> to yield O adatoms, but they usually perturb the electronic structures of co-adsorbed substrate and finally they burn the organic molecules to carbon dioxide and water [6,7]. Supported IL gold nanoparticles could adsorb O<sub>2</sub> and organic molecule chemically and onset the catalytic reaction. Investigation of gas phase interactions of oxygen molecule with gold clusters exhibited sensitivity to the cluster size and gold charge state [24,25]. The adsorption, activation and dissociation of O<sub>2</sub> can be done by electron pushing and donor/acceptor mechanism in supported gold catalysts [27].

It is supposed that supported IL gold nanocatalysts demonstrate similar mechanism. ILs have an activation role through the formation of intermediates involving hydrogen bond formation between the oxygen atoms and the C-2 hydrogen atom of the imidazolium cation as well as electrostatic interaction between the quaternary nitrogen atom of the imidazolium cation with the C=C in alkenes [17]. Understanding the solvation interactions at a molecular scale is important to quantify relevant molecular-microscopic properties. The energetic level of molecules can be modified by interactions with medium species [30].

Solvent effects are related to various solute-solvent interactions, locally developed in the vicinity of the solutes. To study the specific and nonspecific solute-solvent interactions, solvatochromism could be a proper method which is based on UV-Vis spectra band shifts of solvatochromic indicators [31]. In this way, some empirical solvatochromic parameters (SP) including normalized polarity ( $E_T^N$ ), dipolarity/polarizability ( $\pi^*$ ), hydrogen bond donor acidity ( $\alpha$ ) and hydrogen bond acceptor basicity ( $\beta$ )

have been determined to quantify the properties of molecular-microscopic binary solvents [32]. It should be highlighted that EAP demonstrated higher activity compared to [bmim]PF<sub>6</sub> and [emim]EtSO<sub>4</sub>. The reason for this choice arises from the fact that EAP have higher ( $E_T^N$ ),  $\alpha$  and  $\beta$  parameters (Table 3) resulting in more stabilization of intermediates *via* various polarity and hydrogen bonding interactions in oxidation of alkenes. In agreement with the previous works [32,33], it can be suggested that an electron transfer from the support to the metal creates more electron-enriched gold nanoparticles where bonding reaction with the C=C and O=O groups occurs. It seems that direct interaction of the IL with support and gold particles is responsible for this amplifying effect. Hydrogen bond induced reactivity and selectivity control in the imidazolium based ionic liquid catalyzed reactions [14]. Atomic oxygens are preferably adsorbed on the fcc site of Au(111). Deng *et al.* [34] in their experimental study pointed out that there will be O<sub>2</sub> dissociation when the Au(111) surface is mainly precovered by oxygen atom.

## CONCLUSIONS

Selective oxidation of alkenes was investigated using molecular oxygen under mild conditions in the presence of supported gold nanocatalysts. The IL/Au/TiO<sub>2</sub> and IL/Au/Al<sub>2</sub>O<sub>3</sub> catalysts in three phases were applied for the aerobic oxidation. EAP/Au/Al<sub>2</sub>O<sub>3</sub> exhibited maximum conversion compared to the other IL-impregnated catalysts. Supported ionic liquids gold nanocatalysts are active catalysts for oxidation reaction with high efficiency and selectivity.

## REFERENCES

- [1] Xia, Y.; Xiong, Y.; Lim, B.; Skrabalak, S. E., Shape-controlled synthesis of metal nanocrystals: simple chemistry meets complex physics? *Angew. Chem. Int. Ed.* **2009**, *48*, 60-103. DOI: 10.1002/anie.200802248
- [2] Wiley, B.; Sun, Y.; Xia, Y., Synthesis of silver nanostructures with controlled shapes and properties. *Acc. Chem. Res.* **2007**, *40*, 1067-1076. DOI: 10.1021/ar7000974.
- [3] Herricks, T.; Chen, J.; Xia, Y., Polyol synthesis of platinum nanoparticles: control of morphology with sodium nitrate. *Nano Lett.* **2004**, *4*, 2367-2371. DOI: 10.1021/nl048570a.
- [4] Pastoriza-Santos, I.; Liz-Marzán, L. M., N,N-dimethylformamide as a reaction medium for metal nanoparticle synthesis. *Adv. Funct. Mater.* **2009**, *19*, 679-688. DOI: 10.1002/adfm.200801566.
- [5] Sun, Y.; Mayers, B.; Herricks, T.; Xia, Y., Polyol synthesis of uniform silver nanowires: a plausible growth mechanism and the supporting evidence. *Nano Lett.* **2003**, *3*, 955-960. DOI: 10.1021/nl034312m.
- [6] Wiley, B.; Sun, Y.; Mayers, B.; Xia, Y., Shape-controlled synthesis of metal nanostructures: the case of silver. *Chem. A Euro. J.* **2005**, *11*, 454-463. DOI: 10.1002/chem.200400927.
- [7] Xia, Y.; Li, W.; Cogley, C. M.; Chen, J.; Xia, X.; Zhang, Q.; Yang, M.; Cho, E. C.; Brown, P. K., Gold nanocages: from synthesis to theranostic applications. *Acc. Chem. Res.* **2011**, *44*, 914-924. DOI: 10.1021/ar200061q.
- [8] Salari, H.; Harifi-Mood, A. R.; Elahifard, M. R.; Gholami, M. R., Solvatochromic probes absorbance behavior in mixtures of 2-hydroxy ethylammonium formate with methanol, ethylene glycol and glycerol. *J. Sol. Chem.* **2010**, *39*, 1509-1519. DOI: 10.1007/s10953-010-9596-8.
- [9] Salari, H.; Khodadadi-Moghaddam, M.; Harifi-Mood, A. R.; Gholami, M. R., Preferential solvation and behavior of solvatochromic indicators in mixtures of an ionic liquid with some molecular solvents. *J. Phys. Chem. B.* **2010**, *114*, 9586-9593. DOI: 10.1021/jp103476a.
- [10] Salari, H.; Ahmadvand, S.; Harifi-Mood, A. R.; Padervand, M.; Gholami, M. R., Molecular-microscopic properties and preferential solvation in protic ionic liquid mixtures. *J. Sol. Chem.* **2013**, *42*, 1757-1769. DOI: 10.1007/s10953-013-0079-6.
- [11] Salari, H.; Harifi-Mood, A. R.; Elahifard, M. R.; Gholami, M. R., Solvatochromic probes absorbance behavior in mixtures of 2-hydroxy ethylammonium formate with methanol, ethylene glycol and glycerol. *J. Sol. Chem.* **2010**, *39*, 1509-1519. DOI: 10.1007/s10953-010-9596-8.
- [12] Sarkar, A.; Roy, S. R.; Parikh, N.; Chakraborti, A. K., Nonsolvent application of ionic liquids: organocatalysis by 1-alkyl-3-methylimidazolium cation based room-temperature ionic liquids for chemoselective N-tert-butyloxycarbonylation of amines and the influence of the C-2 hydrogen on catalytic efficiency. *J. Org. Chem.* **2011**, *76*, 7132-7140. DOI: 10.1039/B807572G.
- [13] Roy, S. R.; Jadhavar, P. S.; Seth, K.; Sharma, K. K.; Chakraborti, A. K., Organocatalytic application of ionic liquids:[bmim][MeSO<sub>4</sub>] as a recyclable organocatalyst in the multicomponent reaction for the preparation of dihydropyrimidinones and-thiones. *Synthesis* **2011**, *2011*, 2261-2267. DOI: 10.1055/s-0030-1260067.
- [14] Sarkar, A.; Roy, S. R.; Chakraborti, A. K., Ionic liquid catalysed reaction of thiols with  $\alpha,\beta$ -unsaturated carbonyl compounds-remarkable influence of the C-2 hydrogen and the anion. *Chem. Commun.* **2011**, *47*, 4538-4540. DOI: 10.1039/C1CC10151J.
- [15] Roy, S. R.; Chakraborti, A. K., Supramolecular assemblies in ionic liquid catalysis for aza-Michael reaction. *Org. Lett.* **2010**, *12*, 3866-3869. DOI: 10.1021/ol101557t.
- [16] Chakraborti, A. K.; Roy, S. R., On catalysis by ionic liquids. *J. Am. Chem. Soc.* **2009**, *131*, 6902-6903. DOI: 10.1021/ja900076a.
- [17] Chakraborti, A. K.; Roy, S. R.; Kumar, D.; Chopra, P., Catalytic application of room temperature ionic liquids:[bmim][MeSO<sub>4</sub>] as a recyclable catalyst for synthesis of bis (indolyl) methanes. Ion-fishing by MALDI-TOF-TOF MS and MS/MS studies to probe the proposed mechanistic model of catalysis. *Green Chem.* **2008**, *10*, 1111-1118. DOI: 10.1039/

- B807572G.
- [18] Fakhraee, M.; Zandkarimi, B.; Salari, H.; Gholami, M. R., Hydroxyl-functionalized 1-(2-hydroxyethyl)-3-methyl imidazolium ionic liquids: thermodynamic and structural properties using molecular dynamics simulations and ab initio calculations. *J. Phys. Chem. B.* **2014**, *118*, 14410-14428. DOI: 10.1021/jp5083714.
- [19] Huang, X.; Neretina, S.; El-Sayed, M. A., Gold nanorods: from synthesis and properties to biological and biomedical applications. *Adv. Mater.* **2009**, *21*, 4880-4910. DOI: 10.1002/adma.200802789.
- [20] Jana, N. R.; Gearheart, L.; Murphy, C. J., Wet chemical synthesis of high aspect ratio cylindrical gold nanorods. *J. Phys. Chem. B.* **2001**, *105*, 4065-4067. DOI: 10.1021/jp0107964.
- [21] Nikoobakht, B.; El-Sayed, M. A., Preparation and growth mechanism of gold nanorods (NRs) using seed-mediated growth method. *Chem. Mater.* **2003**, *15*, 1957-1962. DOI: 10.1021/cm0207321.
- [22] Pérez-Juste, J.; Pastoriza-Santos, I.; Liz-Marzán, L. M.; Mulvaney, P., Gold nanorods: synthesis, characterization and applications. *Coord. Chem. Rev.* **2005**, *249*, 1870-1901. DOI: 10.1016/j.ccr.2005.01.030.
- [23] Murphy, C. J.; Gole, A. M.; Hunyadi, S. E.; Stone, J. W.; Sisco, P. N.; Alkilany, A.; Kinard, B. E.; Hankins, P., Chemical sensing and imaging with metallic nanorods. *Chem. Commun.* **2008**, *5*, 544-557. DOI: 10.1039/B711069C.
- [24] Yu, C.; Irudayaraj, J., Multiplex biosensor using gold nanorods. *Anal. Chem.* **2007**, *79*, 572-579. DOI: 10.1021/ac061730d.
- [25] Huang, X.; El-Sayed, I. H.; Qian, W.; El-Sayed, M. A., Cancer cell imaging and photothermal therapy in the near-infrared region by using gold nanorods. *J. Am. Chem. Soc.* **2006**, *128*, 2115-2120. DOI: 10.1021/ja057254a.
- [26] Parab, H. J.; Jung, C.; Lee, J. -H.; Park, H. G., A gold nanorod-based optical DNA biosensor for the diagnosis of pathogens. *Biosensors & Bioelectronics* **2010**, *26*, 667-673. DOI: 10.1016/j.bios.2010.06.067.
- [27] Wang, X.; Li, Y.; Wang, H.; Fu, Q.; Peng, J.; Wang, Y.; Du, J.; Zhou, Y.; Zhan, L., Gold nanorod-based localized surface plasmon resonance biosensor for sensitive detection of hepatitis B virus in buffer, blood serum and plasma. *Biosensors & Bioelectronics* **2010**, *26*, 404-410. DOI: 10.1016/j.bios.2010.07.121.
- [28] Sarkar, A.; Trivedi, S.; Pandey, S., Unusual solvatochromism within 1-butyl-3-methylimidazolium hexafluorophosphate + poly (ethylene glycol) mixtures. *J. Phys. Chem. B.* **2008**, *112*, 9042-9049. DOI: 10.1021/jp802833f.
- [29] Habibi-Yangjeh, A.; Jafari-Tarzanag, Y.; Banaei, A. R., Solvent effects on kinetics of an aromatic nucleophilic substitution reaction in mixtures of an ionic liquid with molecular solvents and prediction using artificial neural networks. *Int. J. Chem. Kinet.* **2009**, *41*, 153-159. DOI: 10.1002/kin.20386.
- [30] Singh, A. K.; Senapati, D.; Wang, S.; Griffin, J.; Neely, A.; Naylor, K. M.; Varisli, B.; Kalluri, J. R.; Ray, P. C., Gold nanorod based selective identification of Escherichia coli bacteria using two-photon Rayleigh scattering spectroscopy. *ACS Nano.* **2009**, *3*, 1906-1912. DOI: 10.1021/nn9005494.
- [31] Sudeep, P.; Joseph, S. S.; Thomas, K. G., Selective detection of cysteine and glutathione using gold nanorods. *J. Am. Chem. Soc.* **2005**, *127*, 6516-6517. DOI: 10.1021/ja051145e.
- [32] Turner, M.; Golovko, V. B.; Vaughan, O. P.; Abdulkin, P.; Berenguer-Murcia, A.; Tikhov, M. S.; Johnson, B. F.; Lambert, R. M., Selective oxidation with dioxygen by gold nanoparticle catalysts derived from 55-atom clusters. *Nature* **2008**, *454*, 981. DOI: 10.1038/nature07194.
- [33] Hughes, M. D.; Xu, Y.-J.; Jenkins, P.; McMorn, P.; Landon, P.; Enache, D. I.; Carley, A. F.; Attard, G. A.; Hutchings, G. J.; King, F., Tunable gold catalysts for selective hydrocarbon oxidation under mild conditions. *Nature* **2005**, *437*, 1132. DOI: 10.1038/nature04190.
- [34] Deng, X.; Min, B. K.; Guloy, A.; Friend, C. M., Enhancement of O<sub>2</sub> dissociation on Au(111) by adsorbed oxygen: Implications for oxidation catalysis. *J. Am. Chem. Soc.* **2005**, *127*, 9267-9270. DOI: 10.1021/ja050144j.